

## Polymer-Relief Microstructures by Inkjet Etching\*\*

By Berend-Jan de Gans, Stephanie Hoepfener, and Ulrich S. Schubert\*

Inkjet printing is developing at a rapid pace. The last decade saw continuous improvements in quality and resolution, and the technology has now arrived at the point where it challenges conventional silver halide photography. But inkjet technology is not only a printing technology. A lot of effort is being put into turning inkjet printing into a versatile tool for various industrial processes for accurately depositing minute quantities of materials in defined spots on surfaces, in particular in plastic electronics and polymer light-emitting diodes.<sup>[1–5]</sup> Inkjet printing may also become a cost-saving alternative to photolithography for the production of next-generation active-matrix liquid-crystal displays.<sup>[6]</sup> Of particular interest is the use of inkjet printing in the fields of biotechnology and combinatorial chemistry as a tool for the preparation of inkjet-printed polymer microarrays or libraries,<sup>[7]</sup> i.e., arrays of individually addressable dots or rectangles with well-known compositions on substrates.

Rather than depositing a functional component, an inkjet-printed solvent droplet can also be used to site-selectively remove material that was deposited previously by a different technique.<sup>[8,9]</sup> Via holes were etched in an insulating layer of poly(vinyl phenol) (PVP) by inkjet printing droplets of ethanol, which is known to be a good solvent for PVP. The ethanol locally dissolves the PVP. As a result, a craterlike hole is formed by redeposition of the dissolved polymer at the contact line. The mechanism behind the formation process of the hole is commonly known as the coffee-ring effect. It refers to the formation of a ringlike deposit of solute from a drying droplet by assuming a maximum in the evaporation rate at the outside of the droplet and pinning of the three-phase contact line.<sup>[10–12]</sup> The potential of this “inkjet-etching” technique is evident for any area of technology that uses polymer-relief

microstructures, whereby a more direct structuring technique can be applied than in common photolithographic approaches. The spreading and the minimum diameter of the inkjet-printed droplets, which in recent years could be decreased to less than 10  $\mu\text{m}$ , set the resolution. Even if inkjet etching may not be feasible for production, since it is not as fast as conventional production technologies such as screen printing, the combination of low cost and flexibility makes it an ideal candidate for rapid-prototyping applications. Inkjet etching also holds enormous potential for the production of biochips and micropatterned cell arrays where one single process step suffices to create an immobilizing structure that can be subsequently used to dispense various types of biological matter, bioactive molecules, or even cells.<sup>[13–17]</sup>

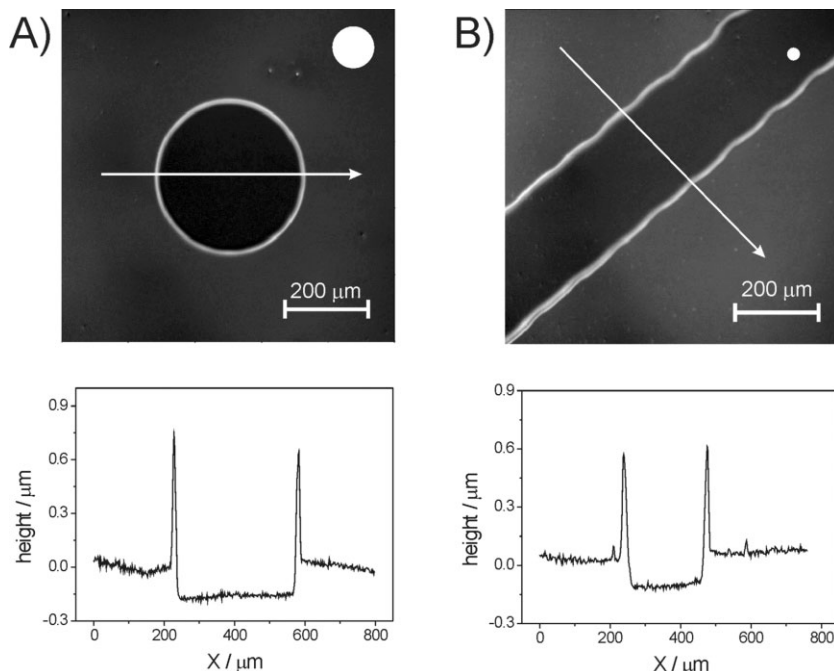
In this paper we report on the investigation of different types of structures that can be created by inkjet etching. The resulting structures are investigated as a function of the etchant, the polymer, and the deposition pattern formed by the solvent droplets. In particular, it will be demonstrated that it is possible to extend the technique to the etching of geometries other than simple holes sometimes with unexpected symmetry. This can be achieved by variation of the spacing between the printed droplets. These structures can then act as reservoirs for other inkjet-printed matter, and a representative example of such a filling process is demonstrated. This discussion includes a detailed nanoscopic investigation of the structure of the holes using scanning force microscopy (SFM).

Figure 1A shows a hole etched in polystyrene using isopropyl acetate to locally dissolve the polymer material. The white circle in the upper right shows the size (to scale) of the solvent droplet ejected by the inkjet printer that produces this hole; the diameter of the droplet is a factor of three smaller than that of the hole it etches. The solvent droplet wets the polymer film and forms a thin fluid film with a circular footprint and a thickness of a few micrometers, assuming that the diameter of the film equals the diameter of the resulting etching hole. This solvent film is responsible for the local dissolution of the polymer material. The bottom of the hole is flat within the resolution of the confocal scanning microscope, indicating that the solvent droplet completely penetrates the polymer layer. The cross section indicates two sharp peaks that mark the edge of each hole (Fig. 1). A careful analysis of these structures reveals a conservation of the total polymer mass. Numerical calculation of  $\int [h(r) - h_0] r dr$  (where  $h$  is the height of the profile shown in Fig. 1 and  $r$  is the distance to the hole center) yields zero within one percent of the hole volume. Here,  $h_0$  denotes the height of the untreated film. When the

[\*] Prof. U. S. Schubert, Dr. B.-J. de Gans, Dr. S. Hoepfener  
Laboratory of Macromolecular Chemistry and Nanoscience  
Eindhoven University of Technology  
and Dutch Polymer Institute (DPI)  
PO Box 513, 5600 MB Eindhoven (The Netherlands)  
E-mail: u.s.schubert@tue.nl

Prof. U. S. Schubert, Dr. S. Hoepfener  
Center for NanoScience, Photonics and Optoelectronic Group  
Ludwig-Maximilians-Universität  
Geschwister-Scholl-Platz 1, 80539 München (Germany)

[\*\*] The research of Berend-Jan de Gans forms part of the research program of the Dutch Polymer Institute (DPI). The authors thank NWO (VICI award for USS) and the Fond der Chemischen Industrie for financial support.



**Figure 1.** A) Confocal scanning microscopy image of a hole etched into a polystyrene film by a 100  $\mu\text{m}$  droplet of isopropyl acetate (shown to scale as the white circle in the upper right). B) Groove etched in poly(benzyl methacrylate) layer by a line of 30  $\mu\text{m}$  *n*-butyl acetate droplets (circle, upper right) with a spacing of 120  $\mu\text{m}$ .

distance between the droplets is reduced, they eventually merge on the substrate and form a line of liquid. This can be used to etch, for example, a groove.<sup>[18]</sup> A typical example, shown in Figure 1B, was obtained using a poly(benzyl methacrylate) layer and *n*-butyl acetate as an etchant.

The size of a hole or groove is expected to depend on a combination of three factors: the spreading of the solvent on the chosen substrate, the rate of evaporation of the solvent, and the rate of dissolution of the polymer. We investigated the size of the hole formed in a polystyrene film using a number of good solvents for polystyrene: ethyl acetate, isopropyl acetate, *n*-butyl acetate, toluene, anisole, and acetophenone. The results are shown in Figure 2. No clear trend can be ob-

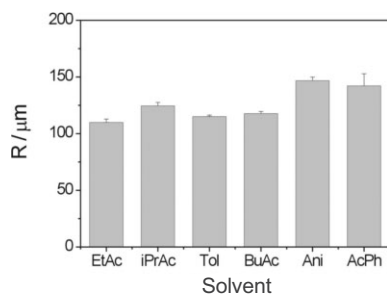


**Figure 2.** Outer radius of holes etched in a polystyrene film using various solvents: ethyl acetate (EtAc), isopropyl acetate (iPrAc), toluene (Tol), *n*-butyl acetate (BuAc), anisole (Ani), and acetophenone (AcPh). The boiling points of the solvents increase from left to right.

served, even if the vapor pressure of anisole (3.51 mm Hg; 1 mm Hg  $\sim$  133 Pa) is ten times larger than the vapor pressure of acetophenone (0.35 mm Hg); the vapor pressure is expected to influence the hole-etching process in terms of the very different evaporation speeds of the solvents. Nonetheless, the sizes of the holes are equal within the experimental error. Apparently, the rate of dissolution always exceeds the rate of evaporation for the polymer/solvent combinations we used, so that the spreading of the solvent on the polystyrene film is the only factor that determines the hole size.

Focusing on possible applications of this structuring technique, it is of utmost importance that, if possible, a large variety of different hole geometries is accessible. We found that inkjet etching provides some unique additional possibilities. A typical example is shown in Figure 3A. The structure thus formed consists of a rectangular pattern that was obtained by printing a rectangular array of acetophenone droplets at a mutual distance of 500  $\mu\text{m}$  using a 70  $\mu\text{m}$  nozzle. Individual cells are rectangular rather than round. Another example is shown in Figure 3B. In this case, a hexagonal

array of droplets was printed at a mutual distance of 150  $\mu\text{m}$  using a 30  $\mu\text{m}$  nozzle. As a result, the holes have a more hexagonal, honeycomblike shape. These unusual shapes of the holes depend strongly on the distance between the solvent drops as deposited on the polymer film. When the distance between the droplets is increased, an array of circular holes is obtained. When the distance is decreased, the droplets merge on the surface and macroscopic, rectangular holes form. The formation of complex shapes of the kind shown in Figure 3 only occurs within a narrow interval of interdroplet distances, typically within a range of only 10  $\mu\text{m}$ .

As the shape of the etched structure always reflects the shape of the etchant during the etching process, these structures are certainly the result of the deformation of adjacent droplets. As evaporation of the solvent droplets occurs on a timescale of seconds—typically one order of magnitude slower than the rate of deposition through the inkjet dispenser—droplet deformation is likely to originate from a repulsive interaction between droplets that suppresses coalescence. Repulsion may originate from the rapid evaporation of solvent due to the high surface-to-volume ratio of the droplets and the resulting flux of solvent vapor, or from the thermal-gradient-driven Marangoni convection inside the droplets, causing a repulsive air flow between them.<sup>[19]</sup> Even if the precise nature of this repulsive interaction remains unknown, it offers a variety of possibilities to manipulate the hole shape, offering solutions for any application that requires a dense packing of cells on a certain area, such as in display fabrication.

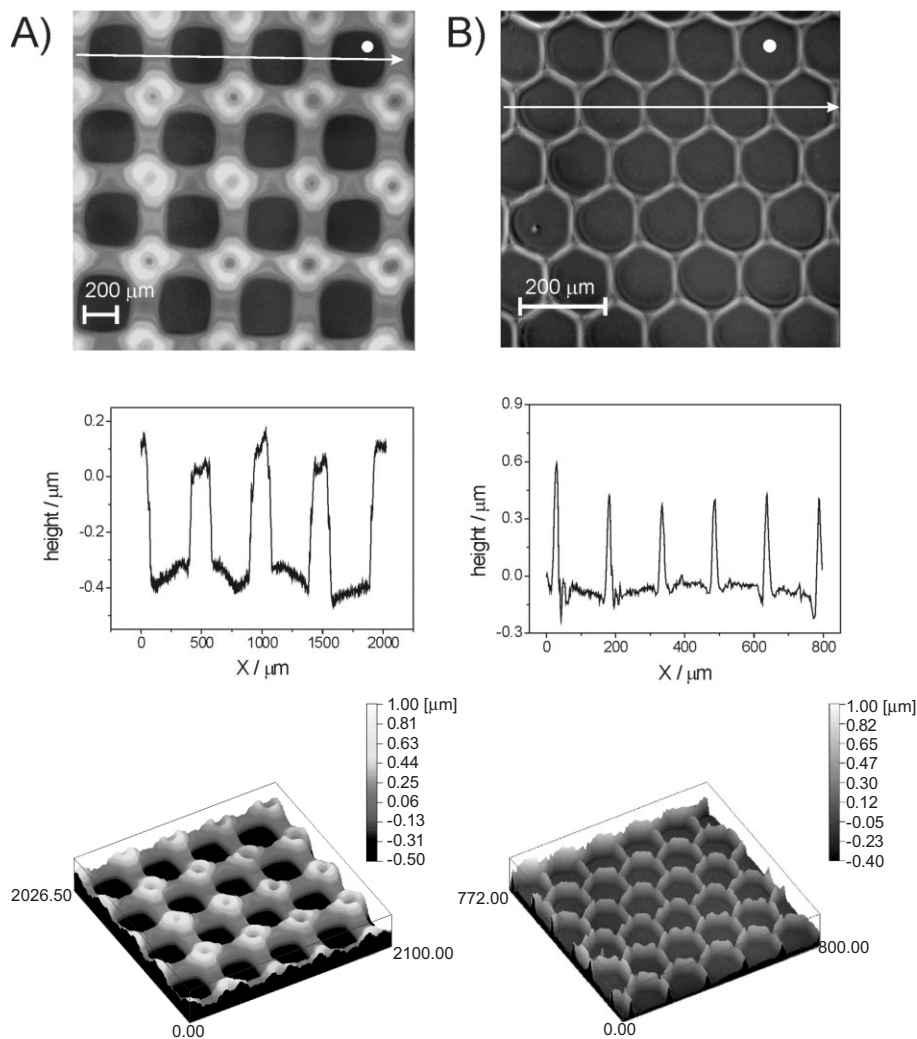


**Figure 3.** A) Rectangular holes etched in polystyrene by a rectangular array of 70  $\mu\text{m}$  acetophenone droplets (shown to scale as the white circle in the upper right). From top to bottom: height map, profile, and 3D image. B) Hexagonal holes etched by a hexagonal array of 30  $\mu\text{m}$  isopropyl acetate droplets.

Etched structures can be used as templates for the deposition of different materials or as small reservoirs for biologically and/or technologically relevant materials, demonstrated here using a dispersion of quantum dots. These quantum dots can easily be discerned from the surrounding polymer using fluorescence microscopy due to their luminescent properties. First, a rectangular array of holes was etched in a polystyrene layer. Second, an aqueous dispersion of CdSe/ZnS core/shell quantum dots was printed into the holes. Figure 4A shows a phase-contrast microscopy image of the resulting structure. The ring surrounding the central hole is clearly observed. A fluorescence microscopy image of the same area is shown in Figure 4B. A single ring of quantum dots forms per hole, the diameter of which is about one-third of the diameter of the polymer ring. This indicates that a secondary polystyrene film is still present in the hole (or, at least, some parts of it); other-

wise, the aqueous dispersion would have wetted the underlying glass completely, and the sizes of both rings would have been approximately identical.<sup>[20]</sup>

SFM was used to investigate the hole structure in more detail. Figure 5A depicts a tapping-mode SFM image of a spin-coated polystyrene film before etching. The film is smooth and exhibits only a few small defects. On the contrary, the surface in the middle of a hole (Fig. 5B) is not entirely smooth, and a number of holes are present. The surface texture is comparable to that of the bare glass substrate. Away from the middle of the hole, towards the polymer ring, the surface again resembles a smooth polymer film. To determine its thickness, this remaining film was scratched. Figure 5C shows a tapping-mode SFM image of the scratch border. The corresponding profile (Fig. 5D) reveals a thickness of 25–30 nm, corresponding to a remaining film of undissolved polymer. For some applications, it may be necessary to remove this remaining film to improve electrical contact or adhesion between the underlying substrate and any material that was placed on top of the inkjet-etched polymer film. This could be done by, e.g., a plasma etching.

In summary, we demonstrated the feasibility of inkjet etching to prepare polymer microstructures. When an inkjet-printed solvent droplet hits a polymer surface, it locally dissolves the polymer material. A hole then forms due to the coffee-ring effect. It could be demonstrated that the hole size is independent on

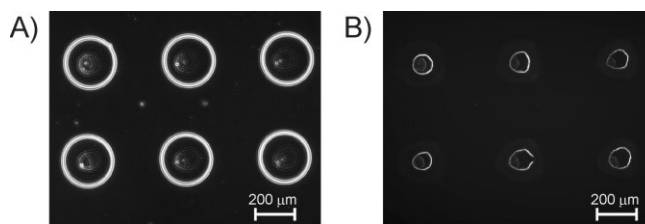


**Figure 4.** A) Phase-contrast microscopy image of a rectangular array of holes etched in polystyrene. An aqueous dispersion of CdSe/ZnS quantum dots was printed inside. B) Fluorescence microscopy image. The quantum dots form a ringlike structure inside the polymer ring.

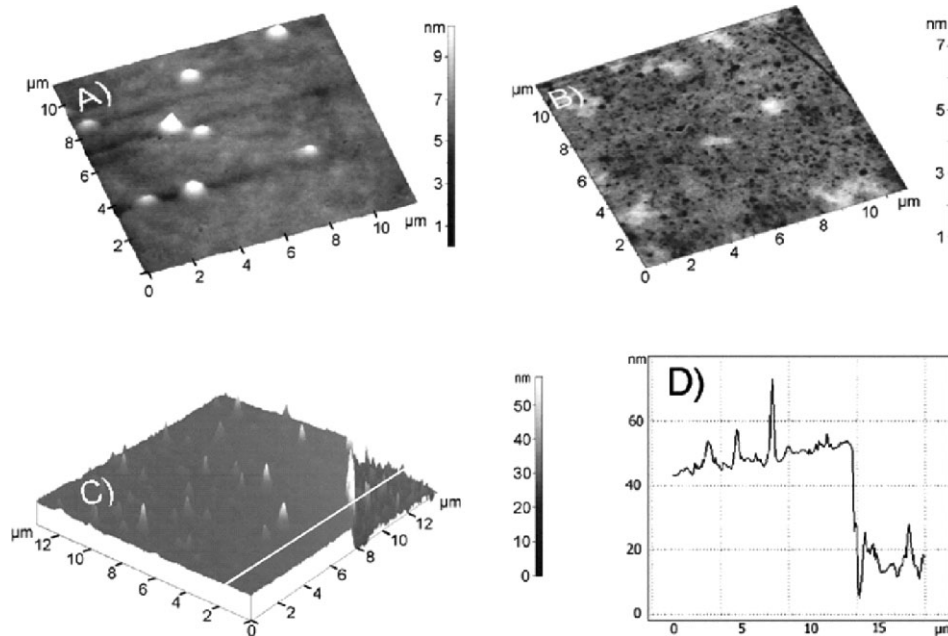


**Figure 5.** A) Tapping-mode SFM image of an untreated spin-coated polystyrene film. B) Morphology at the center of an etched hole. The surface structure is comparable to that of the bare glass substrate. C) Scratched film showing the presence of a secondary polymer film close to the ring around the hole. D) Profile of the scratch shown in (C). Film thickness is 25–30 nm.

the rate of evaporation of the solvent used and thus should depend mainly on its spreading characteristics. The capability of etched structures to act as reservoirs for other materials that can additionally be inkjet printed opens up various possibilities for applications. The formation of dots of deposited material rather than rings suggests only partial removal of the material in the hole structure. This could be confirmed by SFM measurements.

The technique is well-suited for applications in the field of rapid prototyping and the generation of microarrays, but the spectrum of possible applications is additionally broadened by the ability to manipulate the shapes of the holes by adjusting the distance between the individual droplets. This is made possible by a repulsive interaction that deforms the evaporating droplets.

## Experimental

Ethyl acetate and toluene (Biosolve), isopropyl acetate and acetophenone (Sigma–Aldrich), *n*-butyl acetate (Fluka), and anisole (Acros Organics) were filtered through a 5  $\mu\text{m}$  polytetrafluoroethylene filter to remove nozzle-clogging dust particles. Polystyrene (number-average molecular weight  $M_n = 47.0$  kDa; weight-average molecular weight  $M_w = 137.4$  kDa) was purchased from Dow Chemical. Poly(benzyl methacrylate) ( $M_w = 70$  kDa) was purchased from Scientific Polymer Products. Solutions containing 4.0 wt.-% polymer in toluene were prepared by gentle heating and shaking and were filtered before use. Polymer films were spin-cast onto clean microscopy slides using a Suss Microtec RC8 spin-coater. Before use, these slides were treated in a UV–ozone photoreactor (PR-100, UVP) for 30 min. An aqueous dispersion containing 0.25  $\text{mg mL}^{-1}$  CdSe/ZnS quantum dots (EviTags) was purchased from Evident Technologies.

The Autodrop device from Microdrop Technologies was used as an inkjet printer. For a print head, we used several AD-K-501 micropipettes with nozzle diameters of both 30 and 70  $\mu\text{m}$ . The driving signal was a rectangular pulse (width 29  $\mu\text{s}$ , frequency 200 Hz). The amplitude was 70 V for the 70  $\mu\text{m}$  nozzle and 90 V for the 30  $\mu\text{m}$  nozzle. The amplitude and width were chosen to minimize satellite-droplet formation, as this would have caused secondary holes to form. Grooves were etched while printing in flight, i.e., the head moved during printing with a velocity of 6.25  $\text{mm s}^{-1}$ . Arrays were printed with a velocity of 1.25  $\text{mm s}^{-1}$  in between the ejection of two subsequent droplets.

A Nanofocus  $\mu\text{Surf}$  white-light confocal microscope was used to determine the microscopic surface topography. The setup used an external 100 W xenon cold light source and a 20 $\times$  objective. The Nanofocus could also operate as a “normal” microscope and was used as such to determine the sizes of etched holes and lines. Fluorescence microscopy images were obtained with a Zeiss Axiovert 200 M with an excitation wavelength of 555 nm and an FS09 filter. Scanning force microscopy investigations were performed with a NT-MDT Ntegra system in tapping mode using Mikromasch silicon non-contact cantilevers with a typical force constant of 5.5  $\text{N m}^{-1}$ .

Received: September 27, 2005  
Final version: December 17, 2005

- [1] B.-J. de Gans, P. C. Duineveld, U. S. Schubert, *Adv. Mater.* **2004**, *16*, 203.
- [2] H. Sirringhaus, T. Kawase, R. H. Friend, T. Shimoda, M. Inbasekaran, W. Wu, E. P. Woo, *Science* **2000**, *290*, 2123.
- [3] C. W. Sele, T. von Werne, R. H. Friend, H. Sirringhaus, *Adv. Mater.* **2005**, *17*, 997.
- [4] E. I. Haskal, M. Büchel, P. C. Duineveld, A. Sempel, P. van de Weijer, *MRS Bull.* **2002**, *27*, 864.
- [5] Y. Yoshioka, P. Calvert, G. E. Jabbour, *Macromol. Rapid Commun.* **2005**, *26*, 238.

- [6] D. B. van Dam, M. P. J. Peeters, C. J. Curling, R. Schroeders, M. A. Verschuuren, in *IS&T NIP20: 2004 Int. Conf. on Digital Printing Technologies*, Society for Imaging Science and Technology, Springfield, MA **1997**, p. 284.
- [7] B. Halford, *Chem. Eng. News* **2004**, 82 (April 25), 41.
- [8] T. Kawase, H. Siringhaus, R. H. Friend, T. Shimoda, *Adv. Mater.* **2001**, 13, 1601.
- [9] H. Siringhaus, R. H. Friend, T. Kawase, *WO Patent Application 01/47044 A2*, **2001**.
- [10] R. D. Deegan, O. Bakajin, T. F. Dupont, G. Huber, S. R. Nagel, T. A. Witten, *Nature* **1997**, 389, 827.
- [11] R. D. Deegan, O. Bakajin, T. F. Dupont, G. Huber, S. R. Nagel, T. A. Witten, *Phys. Rev. E: Stat., Nonlinear, Soft Matter Phys.* **2000**, 62, 756.
- [12] R. D. Deegan, *Phys. Rev. E: Stat., Nonlinear, Soft Matter Phys.* **2000**, 61, 475.
- [13] J. Hyun, H. Ma, Z. Zhang, T. P. Beebe, Jr., A. Chilkoti, *Adv. Mater.* **2003**, 15, 576.
- [14] J. Alper, *Science* **2004**, 305, 1895.
- [15] T. Xu, S. Petridou, E. H. Lee, E. A. Roth, N. R. Vyavahare, J. J. Hickman, T. Boland, *Biotechnol. Bioeng.* **2004**, 85, 29.
- [16] E. A. Roth, T. Xu, M. Das, C. Gregory, J. J. Hickman, T. Boland, *Biomaterials* **2004**, 25, 3707.
- [17] T. Xu, J. Jin, C. Gregory, J. J. Hickman, T. Boland, *Biomaterials* **2005**, 26, 93.
- [18] T. Kawase, *WO Patent Application 02/33 740 A1*, **2002**.
- [19] P. dell'Aversana, J. R. Banavar, J. Koplik, *Phys. Fluids* **1996**, 8, 15.
- [20] B.-J. de Gans, U. S. Schubert, *Langmuir* **2004**, 20, 7789.